



Published in final edited form as:

Stroke. 2013 December ; 44(12): 3522–3528. doi:10.1161/STROKEAHA.113.002904.

Inhibition of the Sur1-Trpm4 Channel Reduces Neuroinflammation and Cognitive Impairment in Subarachnoid Hemorrhage

Cigdem Tosun, BS, David B. Kurland, BA, Rupal Mehta, MD, Rudy J. Castellani, MD, Joyce L. deJong, DO, Min Seong Kwon, PhD, Seung Kyoon Woo, PhD, Volodymyr Gerzanich, MD, PhD, and J. Marc Simard, MD, PhD

Departments of Neurosurgery (C.T., D.B.K., M.S.K., S.K.W., V.G., J.M.S.), Pathology (R.M., R.J.C., J.M.S.), and Physiology (J.M.S.), University of Maryland School of Medicine, Baltimore; and Department of Pathology, Western Michigan University School of Medicine, Kalamazoo, MI (J.L.d.J.)

Abstract

Background and Purpose—Subarachnoid hemorrhage (SAH) can leave patients with memory impairments that may not recover fully. Molecular mechanisms are poorly understood, and no treatment is available. The sulfonyleurea receptor 1–transient receptor potential melastatin 4 (Sur1-Trpm4) channel plays an important role in acute central nervous system injury. We evaluated upregulation of Sur1-Trpm4 in humans with SAH and, in rat models of SAH, we examined Sur1-Trpm4 upregulation, its role in barrier dysfunction and neuroinflammation, and its consequences on spatial learning.

Methods—We used Förster resonance energy transfer to detect coassociated Sur1 and Trpm4 in human autopsy brains with SAH. We studied rat models of SAH involving filament puncture of the internal carotid artery or injection of blood into the subarachnoid space of the entorhinal cortex. In rats, we used Förster resonance energy transfer and coimmunoprecipitation to detect coassociated Sur1 and Trpm4, we measured immunoglobulin G extravasation and tumor necrosis α overexpression as measures of barrier dysfunction and neuroinflammation, and we assessed spatial learning and memory on days 7 to 19.

Results—Sur1-Trpm4 channels were upregulated in humans and rats with SAH. In rats, inhibiting Sur1 using antisense or the selective Sur1 inhibitor glibenclamide reduced SAH-induced immunoglobulin G extravasation and tumor necrosis α overexpression. In models with entorhinal SAH, rats treated with glibenclamide for 7 days after SAH exhibited better platform search strategies and better performance on incremental and rapid spatial learning than vehicle-treated controls.

© 2013 American Heart Association, Inc.

Correspondence to J. Marc Simard, MD, PhD, Department of Neurosurgery, 22 S. Greene St, Suite S12D, Baltimore, MD 21201–1595. msimard@smail.umaryland.edu.

The online-only Data Supplement is available with this article at <http://stroke.ahajournals.org/lookup/suppl/doi:10.1161/STROKEAHA.113.002904/-/DC1>.

Disclosures

Dr Simard holds a US patent (7,285,574), a novel nonselective cation-channel in neural cells and methods for treating brain swelling. Dr Simard is a member of the scientific advisory board and holds shares in Remedy Pharmaceuticals. No support, direct or indirect, was provided to Dr Simard, or for this project by Remedy Pharmaceuticals. The other authors report no conflicts.

Conclusions—Sur1-Trpm4 channels are upregulated in humans and rats with SAH. Channel inhibition with glibenclamide may reduce neuroinflammation and the severity of cognitive deficits after SAH.

Keywords

cognition; memory; subarachnoid hemorrhage; sulfonylurea receptor; transient receptor potential melastatin 4

Subarachnoid hemorrhage (SAH) can be devastating. Acutely, 30% of patients die,¹ and those who survive may have poor prognoses.² Among the worst cases are those in which the hemorrhage involves eloquent cortex, a situation frequently encountered with rupture of middle cerebral artery aneurysms.³

SAH is associated with 2 neurological problems long considered to be intractable: cerebral vasospasm and cognitive impairment. Great progress has been made in characterizing molecular mechanisms of vasospasm, with recent clinical trials on endothelin antagonists showing that angiographic vasospasm can be prevented.⁴ By contrast, cognitive impairments including disorders of memory, executive function, and language, although well documented,⁵ are poorly understood molecularly, and no treatment is available.

The adenosine triphosphate (ATP)–binding cassette (ABC) transporters comprise a large superfamily of membrane proteins.^{6,7} Two members, Sur1 and Sur2, coassociate with heterologous pore-forming subunits to form ion channels.⁸ For Sur1, the most widely recognized association is with the ATP-sensitive K⁺ channel, Kir6.2, with which it forms K_{ATP} (Sur1-Kir6.2) channels in pancreatic β cells and neurons. Sur1 also associates with an ATP- and Ca²⁺-sensitive nonselective cat-ion-channel, recently identified as transient receptor potential melastatin 4 (Trpm4), to form Sur1-Trpm4 channels⁹ (previously named Sur1-NC_{CaATP} channels). Both K_{ATP} (Sur1-Kir6.2) and Sur1-Trpm4 channels are regulated by Sur1, but the 2 have opposite functional effects: opening of K_{ATP} channels hyperpolarizes the cell, whereas opening of Sur1-Trpm4 channels depolarizes the cell. Unchecked opening of Sur1-Trpm4 channels is associated with excess influx of Na⁺, which is accompanied by influx of Cl⁻ and H₂O, resulting in oncotic cell swelling (cytotoxic edema) and, if severe, necrotic cell death.^{10,11} Involvement of microvascular endothelium results in the formation of ionic and vasogenic edema.^{12,13}

Sur1 has been implicated in a rat model of SAH, with Sur1 blockade by glibenclamide associated with a significant reduction in several markers of neuroinflammation.¹³ However, demonstrating the involvement of Sur1 leaves unanswered the question of whether K_{ATP} (Sur1-Kir6.2) or Sur1-Trpm4 channels are involved. Recently, an antibody-based method using Förster resonance energy transfer (FRET) was developed that permits the identification of native coassociated Sur1 and Trpm4, signaling the presence of functional Sur1-Trpm4 channels.⁹ FRET, which can be used to detect the coassociation of 2 fluorescent-labeled proteins, occurs when the energy of an excited fluorophore, called the donor, is nonradiatively passed on to an acceptor fluorophore that is in close proximity. Recently, we used FRET to demonstrate Sur1-Trpm4 channels in rat tissues after spinal cord injury.⁹ Here, we show that coassociated Sur1 and Trpm4 can be identified in cortical tissues from patients with SAH, as well as in cortical tissues from a rat model of SAH. In addition, we show that the channel plays a crucial role in blood–brain barrier (BBB) permeability and in neuroinflammation, and we show that in rat models of SAH involving eloquent cortex, blockade of the channel by the selective Sur1 inhibitor, glibenclamide, significantly ameliorates impairments in spatial learning and memory.

Methods

Human Tissues

Tissue collection protocols were approved by the Institutional Review Boards of the University of Maryland, Baltimore, MD, and the Sparrow Hospital, Lansing, MI. The cases of 7 patients dying within several days of acute SAH who underwent autopsy were identified retrospectively. Demographic and other information on these patients is given in Table I in the online-only Data Supplement. Gross and histological validation of the presence of acute SAH was made in all cases by a neuropathologist. Cortex involved in SAH was analyzed.

As negative controls, frontal and parietal cortices from 5 normal autopsy brains with documented absence of SAH, ipsilateral ischemia, or other central nervous system pathology also were examined. Demographic and other information on these patients is given in Table I in the online-only Data Supplement.

As positive controls for K_{ATP} (Sur1-Kir6.2), normal pancreases and hippocampi obtained at autopsy also were evaluated.

Rat Model of SAH

Animal experiments were performed under a protocol approved by the Institutional Animal Care and Use Committee (IACUC) of the University of Maryland. All experiments were performed in accordance with the relevant guidelines and regulations in the United States National Institutes of Health Guide for the Care and Use of Laboratory Animals. All efforts were made to minimize the number of animals used and their suffering.

Male Wistar rats (300–350 g, Harlan, Indianapolis, IN) were anesthetized (ketamine 60 mg/kg and xylazine 7.5 mg/kg intraperitoneally). SpO_2 via pulse oximetry and temperature were carefully regulated, and all surgical procedures were performed aseptically. SAH was produced either by (1) stereotactic injection of fresh non-heparinized autologous tail blood into the subarachnoid space of the entorhinal cortex,¹⁴ except that 150 μ L of blood was injected >20 minutes, either unilaterally or bilaterally; or (2) by filament puncture of the internal carotid artery.¹³ Three series of rats with blood injections into the entorhinal cortex were studied. In series 1, 11 rats underwent entorhinal SAH and were euthanized 24 to 48 hours later for immunohistochemistry, FRET, or coimmunoprecipitation experiments. In series 2, 14 rats underwent unilateral entorhinal SAH and in series 3, 18 rats underwent bilateral entorhinal SAH; for series 2 and 3, half in each series were randomly assigned to vehicle or glibenclamide treatment. On days 7 to 19 after SAH, all were evaluated in the Morris water maze (MWM) by blinded investigators, after which they were euthanized. No rat in series 2 or 3 was excluded. Series 4 consisted of 7 uninjured rats that served as controls for the MWM testing. For Series 5, 6 rats underwent filament puncture of the internal carotid artery and were administered antisense oligodeoxynucleotide (AS-ODN) directed against *Abcc8* or scrambled oligodeoxynucleotide (Scr-ODN; 3 rats per group). The brains of these rats were analyzed at 24 hours for immunoglobulin G extravasation and tumor necrosis α (TNF α) expression.

Glibenclamide Treatment

Drug formulation of glibenclamide (#G2539; Sigma, St. Louis, MO) in dimethyl sulfoxide and the preparation of miniosmotic pumps were as described.¹⁵ Treatment consisted of (1) administering a single loading dose of glibenclamide (10 μ g/kg) or an equivalent volume of vehicle IP within 10 minutes of completing the injection(s) of blood; (2) continuous infusion via miniosmotic pump (Alzet 2001, 1.0 μ L/hr; Alzet Corp, Cupertino, CA) beginning at the

end of surgery, resulting in delivery of 200 ng/hr or an equivalent volume of vehicle subcutaneously for 1 week. The dose of glibenclamide used here has been shown to not result in hypoglycemia.¹⁰

Antisense Treatment

AS-ODN directed against *Abcc8* and Scr-ODN were prepared and administered IV via miniosmotic pump as described,¹⁶ starting within 10 minutes of SAH and continuing for 24 hours.

Histochemistry and FRET

Immunohistochemistry and antibody-based FRET were performed using custom anti-Sur1 and anti-Trpm4 antibodies, as described,⁹ except that FRET imaging and measurements of FRET efficiency were performed using a Zeiss LSM710 confocal microscope. Semiquantitative analysis of immunolabeling for Sur1, which was used as a proxy for Sur1-Trpm4 channels, was performed as described.¹⁷ Quantitative analyses of immunoglobulin G (1:200; Santa Cruz Biotechnology) and TNF α (1:100; Santa Cruz Biotechnology) immunolabeling in cortex adjacent to SAH, Black Gold II (Millipore, Temecula, CA) labeling of perforant pathway, Fluoro-Jade C staining (Histo-Chem, Jefferson, AR) of hippocampus, and 4',6-diamidino-2-phenylindole (DAPI; Invitrogen, Eugene, OR) labeling of pyknotic nuclei in the dentate gyrus were performed as described.^{13,14}

Coimmunoprecipitation

Coimmunoprecipitation and immunoblot were performed using custom anti-Sur1 and anti-Trpm4 antibodies, as described.⁹

Morris Water Maze

MWM learning took place on days 7 to 11 after SAH using the device and the paradigms described.¹⁸ The memory probe was performed on day 12, and rapid learning was tested on day 19 after SAH. Platform search strategies were analyzed according to Brody and Holtzman.¹⁹ Investigators evaluating MWM performance were blinded to treatment group.

Data Analysis

Data are presented as mean \pm SE. Statistical analyses were performed using Origin Pro (V8; OriginLab Corp, North Hampton MA). Student *t* test, 1-way ANOVA, or repeated measures ANOVA with Fisher post hoc comparisons were used, as appropriate.

Results

Sur1-Trpm4 in Humans With SAH

We used antibody-based FRET to study the coassociation of Sur1 with a pore-forming subunit, either Kir6.2 or Trpm4.⁹ We first validated the method of FRET using COS-7 cells heterologously expressing Sur1 and Trpm4 (Figure I in the online-only Data Supplement) and human and rat pancreas, which expresses K_{ATP} channels, that is, coassociated Sur1 and Kir6.2 (Figure II in the online-only Data Supplement).²⁰ In all cases, Sur1 was found by FRET to coassociate with the pore-forming subunit, either Kir6.2 or Trpm4, whereas appropriate controls did not show FRET.

We studied cortical tissues of patients who were verified at autopsy to have SAH from a ruptured saccular aneurysm or another cause (Table I in the online-only Data Supplement). Cortex adjacent to SAH showed prominent upregulation of Sur1 (Figure 1A and 1B) compared with control cortex (Figure III in the online-only Data Supplement). Similarly,

cortex adjacent to SAH showed prominent upregulation of Trpm4 (Figure 1B) compared with control cortex (Figure III in the online-only Data Supplement). Sur1 and Trpm4 upregulation colocalized to both microvessels and neurons, with FRET analysis demonstrating that the 2 proteins coassociated (Figure 1C). FRET efficiency, which reflects the proximity of the 2 fluorophores, was \approx 11% to 14% in positive controls (COS-7 expression system and human pancreas), 0% in a negative control, and \approx 10% in cortical structures from patients with SAH (Figure 1C). Semiquantitative analysis showed that the abundance of Sur1-Trpm4 channels in microvessels, neurons, and astrocytes varied between cases of SAH, but always exceeded findings in control brains (Table I in the online-only Data Supplement). Sur1 expression is not influenced by postmortem interval.¹⁷

Sur1-Trpm4 in Rats With SAH

Brain tissues from the entorhinal SAH model were studied 24 to 48 hours after SAH. Cortical microvessels, neurons, and astrocytes near the SAH showed expression of both Sur1 and Trpm4, and FRET confirmed that Sur1 and Trpm4 were coassociated (Figure 2A–C). Cortex adjacent to SAH that expressed Sur1 in microvessels and cells exhibited minimal expression of Kir6.2 and no FRET, consistent with absence of K_{ATP} (Figure II in the online-only Data Supplement). Control brains showed little or no immunolabeling for Sur1 or Trpm4 and no FRET (not shown).¹³

The coassociation of Sur1 and Trpm4 demonstrated by FRET was verified by coimmunoprecipitation. Normally, Trpm4 is expressed predominantly in restricted areas of rat brain,²¹ but minimally in cortex (Figure III in the online-only Data Supplement). Compared with uninjured control tissues, there was a 3-fold increase in Trpm4 in tissues adjacent to SAH (Figure 2D). Coimmunoprecipitation using anti-Sur1 antibody for immunoprecipitation revealed an 8-fold increase in coassociated Sur1-Trpm4 (Figure 2D).

Inhibition of Sur1

To assess the downstream consequence of Sur1-Trpm4 channel upregulation, we evaluated the effect of *Abcc8* gene suppression on SAH-induced BBB permeability. A pathological increase in BBB permeability was identified in 2 models of SAH, one with blood injection into the entorhinal cortex, and the other with filament puncture of the internal carotid artery (Figure 3), demonstrating that BBB dysfunction in cortex adjacent to SAH is model independent. AS-ODN directed against *Abcc8* significantly reduced Sur1 expression in cortex adjacent to SAH (Figure 3A), and significantly reduced the SAH-induced abnormality in barrier permeability (Figure 3B). Pharmacological inhibition of Sur1 with glibenclamide was as effective as gene suppression of *Abcc8* in ameliorating barrier dysfunction (Figure 3C).

Extravasation of serum proteins promotes neuroinflammation.²² We evaluated the impact of Sur1 inhibition on SAH-induced overexpression of the acute phase reactant cytokine, TNF α . Both gene suppression of *Abcc8* with antisense and pharmacological inhibition of Sur1 with glibenclamide reduced TNF α expression in adjacent cortical tissues \approx 4-fold (Figure 4), confirming the critical proinflammatory role of Sur1 in SAH.¹³

Spatial Learning and Memory

We used the MWM to assess incremental and rapid spatial learning and memory in rats with either unilateral or bilateral entorhinal SAH that had been administered either glibenclamide or vehicle after SAH.

Rats with unilateral entorhinal SAH performed well overall. Except for the first day of training (day 7 after SAH), when they took longer and used less efficient platform search

strategies, their performance during incremental learning was similar to uninjured naïve control rats (Figure IV in the online-only Data Supplement). Similarly, there was no deficit in the memory probe on day 12 (Figure IV in the online-only Data Supplement). However, rats with unilateral entorhinal SAH treated with vehicle exhibited a significant deficit in rapid spatial learning on day 19 that was largely absent in rats with unilateral entorhinal SAH treated with glibenclamide (Figure IV in the online-only Data Supplement).

Rats with bilateral entorhinal SAH that were administered vehicle performed poorly. They repeatedly took longer to find the platform and used inefficient search strategies, compared with uninjured naïve control rats (Figure 5A and 5B). Both the memory probe on day 12 and the test of rapid learning on day 19 showed that they swam in the correct quadrant no more than a quarter of the time, as expected from chance alone (Figure 5C and 5D). By comparison, rats with bilateral entorhinal SAH administered glibenclamide performed better, with incremental learning on days 7 to 11, platform search strategy on day 11, and memory probe on day 12 being indistinguishable from uninjured naïve control rats (Figure 5A–C). Only in the test of rapid learning on day 19 did glibenclamide-treated rats with bilateral entorhinal SAH exhibit a significant deficit, with their performance not significantly better than vehicle-treated rats (Figure 5D).

Tissue Preservation

Rapid spatial learning is a hippocampus-specific task. We examined the hippocampi, which are physically remote from the entorhinal SAH, but which receive important afferent synaptic input from the entorhinal cortex.²³ Quantitative analyses were performed for Black Gold II labeling of perforant pathway white matter, Fluoro-Jade C staining of hippocampus, and DAPI staining of pyknotic nuclei in the dentate gyrus. As previously reported for this model,¹⁴ these measures of hippocampal injury were present in vehicle controls (Figure 6). Glibenclamide treatment significantly reduced each measure of injury (Figure 6).

Discussion

The major finding of this study is that, in the brains of humans and rats after SAH, but not in controls, coassociated Sur1 and Trpm4 subunits were readily detected, either by FRET or by coimmunoprecipitation, consistent with *de novo* upregulation of Sur1-Trpm4 channels.⁹ In the human cases, available tissues were formalin fixed, precluding coimmunoprecipitation, and so the coassociation of Sur1 and Trpm4 was demonstrated using FRET. In rats, where unfixed tissues were available, coassociation was demonstrated using both FRET and coimmunoprecipitation. Sur1-Trpm4 channels were identified in microvascular endothelium, neurons, and astrocytes. Our previous report identified *de novo* upregulation of Sur1 in a model of SAH,¹³ but that study left unanswered the question of whether Sur1 was associated with Kir6.2 (K_{ATP}), or with Trpm4. The present study provides strong evidence that Sur1-Trpm4, not K_{ATP} , channels are upregulated in cortex adjacent to SAH.

The present study implicates the Sur1-Trpm4 channel in SAH-induced abnormal BBB permeability and neuroinflammation, with blockade of the channel resulting in significant reductions in extravasated serum proteins, TNF α overexpression, and deficits in spatial learning and memory. Vasogenic edema attributable to breakdown of the BBB is widely recognized for its role in brain swelling, but the associated extravasation of serum proteins is underappreciated as a potent cause of neuroinflammation resulting in neuronal dysfunction.²² Available treatments for edema such as osmotherapy may reduce swelling but are unlikely to alter the proinflammatory effects of extravasated proteins. Preventing vasogenic edema by maintaining the integrity of the BBB is preferable to osmotherapy for treating the already swollen brain.

Compared with other pathological effects of SAH, especially vasospasm, there has been a paucity of attention focused on mechanisms of cognitive impairment in animal models of SAH. In the endovascular perforation model, which causes transient global ischemia and $\approx 33\%$ mortality, neurobehavioral consequences are generally unimpressive, with surviving animals having only mild or no abnormalities in MWM testing.²⁴ Models with injection of 250 to 300 μL of blood into the prechiasmatic cistern yield modest abnormalities in MWM testing on days 4 to 5 after SAH^{25,26}; however, to our knowledge, there are no reports of deficits persisting >5 days.

We studied a model designed to affect what is arguably the most eloquent cortex in the rat. The neuronal circuitry involving entorhinal cortices, perforant pathway, and dentate gyrus granule cells plays a critical role in spatial learning,²³ which is readily evaluated in rats using MWM paradigms. We previously showed that SAH (50 μL injection) involving the entorhinal cortex results in demyelination of the perforant pathway and transsynaptic apoptosis of dentate gyrus granule cells, and is associated with neuroinflammation that extended along this pathway into the hippocampus.¹⁴ As predicted by the known function of this neuronal circuitry,²³ here we found that unilateral entorhinal SAH resulted in mild deficits in all spatial learning tasks except rapid spatial learning on day 19, whereas bilateral entorhinal SAH was marked by major deficits in all spatial learning tasks assessed during days 7 to 19 after SAH. Abnormalities in spatial learning and memory in these models were ameliorated by glibenclamide, in concert with better white matter preservation in the perforant pathway and less cell damage and cell death in the hippocampus.

Potential shortcomings of the present study are that the number of human cases examined was small and not all cases were attributable to rupture of a saccular aneurysm. Our focus here was on the presence of blood in the subarachnoid space and the effect of that blood on adjacent cortical cells. In all cases, we observed coassociated Sur1-Trpm4 in nearby cortical microvessels and neurons, despite the variety of causes of SAH. Our findings point to SAH, per se, rather than the pathogenesis of SAH, as the dominant factor that these cases have in common, in keeping with the finding that immunoglobulin G extravasation and TNF α overexpression in the rats were model independent. Obtaining tissues from patients with SAH who survive is ethically unacceptable because removing intact cortical tissues at surgery cannot be justified. However, our parallel work with tissues from the rat models of SAH supports the hypothesis that SAH is associated with upregulation of Sur1-Trpm4 channels⁹ in adjacent cortical tissues and suggests that targeting Sur1-Trpm4 in patients with SAH may be desirable.

Conclusions

We conclude that Sur1-Trpm4 channels are upregulated in humans and rats with SAH, and that channel inhibition with glibenclamide may be useful for reducing neuroinflammation and cognitive deficits after SAH.

Supplementary Material

Refer to Web version on PubMed Central for supplementary material.

Acknowledgments

Sources of Funding

This work was supported by grants to Dr Simard from the National Heart, Lung, and Blood Institute (HL082517) and the National Institute of Neurological Disorders and Stroke (NS061808).

References

1. Hanel RA, Xavier AR, Mohammad Y, Kirmani JF, Yahia AM, Qureshi AI. Outcome following intracerebral hemorrhage and subarachnoid hemorrhage. *Neurol Res.* 2002; 24(suppl 1):S58–S62. [PubMed: 12074438]
2. Quigley MR, Salary M. Defining survivorship after high-grade aneurysmal subarachnoid hemorrhage. *Surg Neurol.* 2008; 69:261–265. [PubMed: 18221774]
3. Niikawa S, Kitajima H, Ohe N, Miwa Y, Ohkuma A. Significance of acute cerebral swelling in patients with sylvian hematoma due to ruptured middle cerebral artery aneurysm, and its management. *Neurol Med Chir (Tokyo).* 1998; 38:844–849. [PubMed: 10063358]
4. Ma J, Huang S, Ma L, Liu Y, Li H, You C. Endothelin-receptor antagonists for aneurysmal subarachnoid hemorrhage: an updated meta-analysis of randomized controlled trials. *Crit Care.* 2012; 16:R198. [PubMed: 23078672]
5. Al-Khindi T, Macdonald RL, Schweizer TA. Cognitive and functional outcome after aneurysmal subarachnoid hemorrhage. *Stroke.* 2010; 41:e519–e536. [PubMed: 20595669]
6. Shi NQ, Ye B, Makielski JC. Function and distribution of the SUR isoforms and splice variants. *J Mol Cell Cardiol.* 2005; 39:51–60. [PubMed: 15978902]
7. Aittoniemi J, Fotinou C, Craig TJ, de Wet H, Proks P, Ashcroft FM. Review. SUR1: a unique ATP-binding cassette protein that functions as an ion channel regulator. *Philos Trans R Soc Lond B Biol Sci.* 2009; 364:257–267. [PubMed: 18990670]
8. Hollenstein K, Dawson RJ, Locher KP. Structure and mechanism of ABC transporter proteins. *Curr Opin Struct Biol.* 2007; 17:412–418. [PubMed: 17723295]
9. Woo SK, Kwon MS, Ivanov A, Gerzanich V, Simard JM. The sulfonylurea receptor 1 (Sur1)-transient receptor potential melastatin 4 (Trpm4) channel. *J Biol Chem.* 2013; 288:3655–3667. [PubMed: 23255597]
10. Simard JM, Woo SK, Schwartzbauer GT, Gerzanich V. Sulfonylurea receptor 1 in central nervous system injury: a focused review. *J Cereb Blood Flow Metab.* 2012; 32:1699–1717. [PubMed: 22714048]
11. Simard JM, Woo SK, Gerzanich V. Transient receptor potential melastatin 4 and cell death. *Pflugers Arch.* 2012; 464:573–582. [PubMed: 23065026]
12. Simard JM, Chen M, Tarasov KV, Bhatta S, Ivanova S, Melnitchenko L, et al. Newly expressed SUR1-regulated NC(Ca-ATP) channel mediates cerebral edema after ischemic stroke. *Nat Med.* 2006; 12:433–440. [PubMed: 16550187]
13. Simard JM, Geng Z, Woo SK, Ivanova S, Tosun C, Melnichenko L, et al. Glibenclamide reduces inflammation, vasogenic edema, and caspase-3 activation after subarachnoid hemorrhage. *J Cereb Blood Flow Metab.* 2009; 29:317–330. [PubMed: 18854840]
14. Simard JM, Tosun C, Ivanova S, Kurland DB, Hong C, Radecki L, et al. Heparin Reduces Neuroinflammation and Transsynaptic Neuronal Apoptosis in a Model of Subarachnoid Hemorrhage. *Transl Stroke. Res.* 2012; 3(suppl 1):155–165. [PubMed: 22707992]
15. Simard JM, Woo SK, Tsybalyuk N, Voloshyn O, Yurovsky V, Ivanova S, et al. Glibenclamide-10-h Treatment Window in a Clinically Relevant Model of Stroke. *Transl Stroke. Res.* 2012; 3:286–295. [PubMed: 22707989]
16. Simard JM, Woo SK, Norenberg MD, Tosun C, Chen Z, Ivanova S, et al. Brief suppression of Abcc8 prevents autodestruction of spinal cord after trauma. *Sci Transl Med.* 2010; 2:28ra29.
17. Mehta RI, Ivanova S, Tosun C, Castellani RJ, Gerzanich V, Simard JM. Sulfonylurea receptor 1 expression in human cerebral infarcts. *J Neuropathol Exp Neurol.* 2013; 72:871–883. [PubMed: 23965746]
18. Patel AD, Gerzanich V, Geng Z, Simard JM. Glibenclamide reduces hippocampal injury and preserves rapid spatial learning in a model of traumatic brain injury. *J Neuropathol Exp Neurol.* 2010; 69:1177–1190. [PubMed: 21107131]
19. Brody DL, Holtzman DM. Morris water maze search strategy analysis in PDAPP mice before and after experimental traumatic brain injury. *Exp Neurol.* 2006; 197:330–340. [PubMed: 16309676]

20. Guiot Y, Stevens M, Marhfour I, Stienet P, Mikhailov M, Ashcroft SJ, et al. Morphological localisation of sulfonylurea receptor 1 in endocrine cells of human, mouse and rat pancreas. *Diabetologia*. 2007; 50:1889–1899. [PubMed: 17593344]
21. Teruyama R, Sakuraba M, Kurotaki H, Armstrong WE. Transient receptor potential channel m4 and m5 in magnocellular cells in rat supraoptic and paraventricular nuclei. *J Neuroendocrinol*. 2011; 23:1204–1213. [PubMed: 21848647]
22. Wagner KR, Dean C, Beiler S, Bryan DW, Packard BA, Smulian AG, et al. Plasma infusions into porcine cerebral white matter induce early edema, oxidative stress, pro-inflammatory cytokine gene expression and DNA fragmentation: implications for white matter injury with increased blood-brain-barrier permeability. *Curr Neurovasc Res*. 2005; 2:149–155. [PubMed: 16181107]
23. Xavier GF, Costa VC. Dentate gyrus and spatial behaviour. *Prog Neuropsychopharmacol Biol Psychiatry*. 2009; 33:762–773. [PubMed: 19375476]
24. Silasi G, Colbourne F. Long-term assessment of motor and cognitive behaviours in the intraluminal perforation model of subarachnoid hemorrhage in rats. *Behav Brain Res*. 2009; 198:380–387. [PubMed: 19059287]
25. Chen G, Li Q, Feng D, Hu T, Fang Q, Wang Z. Expression of NR2B in different brain regions and effect of NR2B antagonism on learning deficits after experimental subarachnoid hemorrhage. *Neuroscience*. 2013; 231:136–144. [PubMed: 23219940]
26. Jeon H, Ai J, Sabri M, Tariq A, Macdonald RL. Learning deficits after experimental subarachnoid hemorrhage in rats. *Neuroscience*. 2010; 169:1805–1814. [PubMed: 20600651]

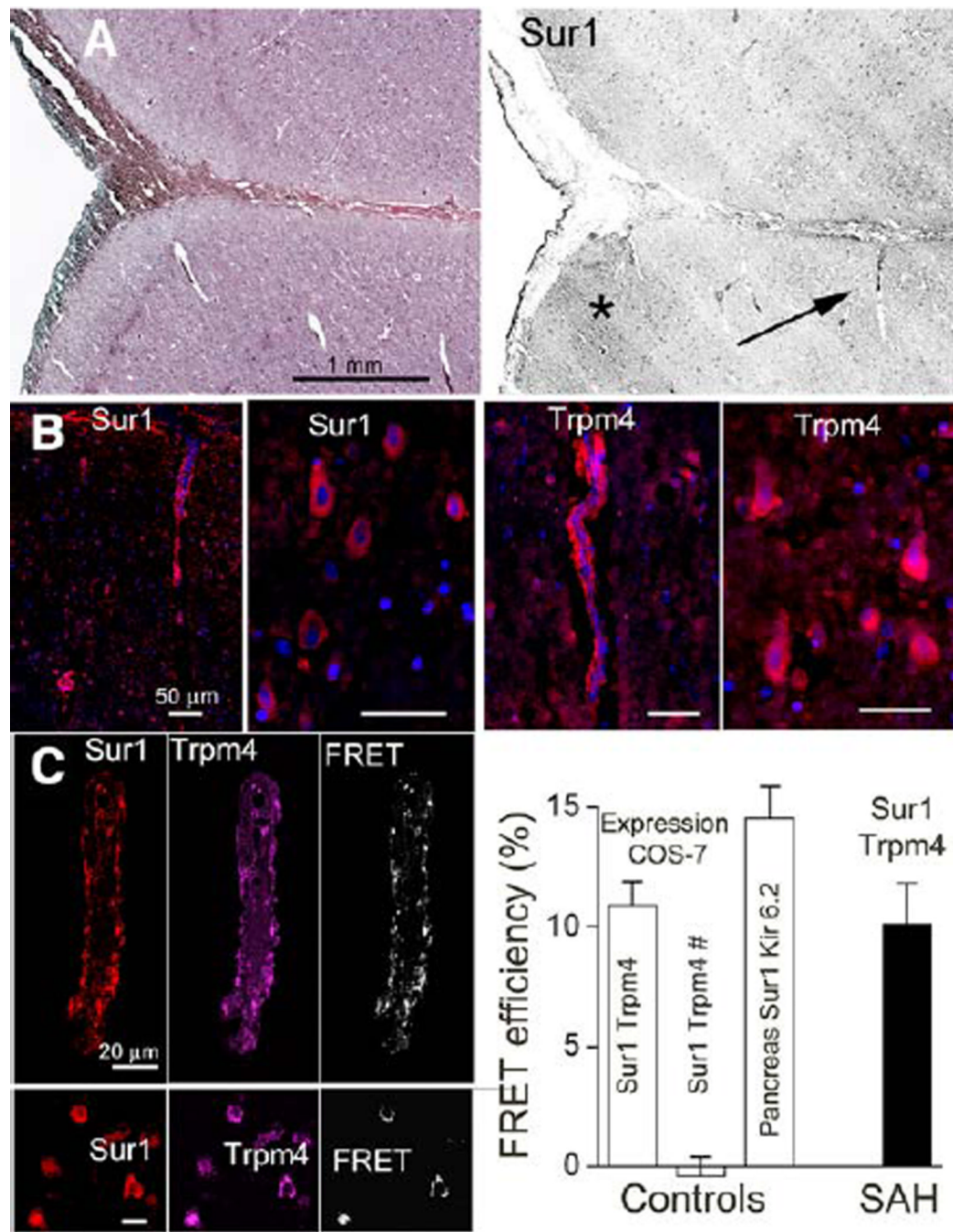


Figure 1.

Sur1-Trpm4 channel in human subarachnoid hemorrhage (SAH) shown by Förster resonance energy transfer (FRET). **A**, H&E-stained section showing SAH (**left**) and adjacent section immunolabeled for Sur1 (**right**; inverse black and white images shown for clarity); arrow: arteriole shown in **B**; asterisk: neurons shown in **B**. **B**, Immunolabeled cortex shows expression of Sur1 and Trpm4 in elongated microvessels and pyramidal neurons. **C**, Coimmunolabeled cortex shows coexpression of Sur1 and Trpm4 and FRET in elongated microvessels and pyramidal neurons (**left**); the bar graph (**right**) shows FRET efficiency for (1) COS-7 cells coexpressing Sur1 and Trpm4, immunolabeled with anti-Trpm4

antibody directed against a cytoplasmic loop and coimmunolabeled with anti-Sur1 antibody directed against either a cytoplasmic loop (Sur1-Trpm4; positive control) or against the extracellular N-terminus (Sur1-Trpm4#; negative control); (2) human pancreas immunolabeled with anti-Sur1 and anti-Kir6.2 antibodies; (3) human brains with SAH immunolabeled with anti-Sur1 and anti-Trpm4 antibodies as in **B** and **C**; n=58 to 64 measurements for COS-7 cells; n=28 to 34 for human pancreas and SAH cortex.

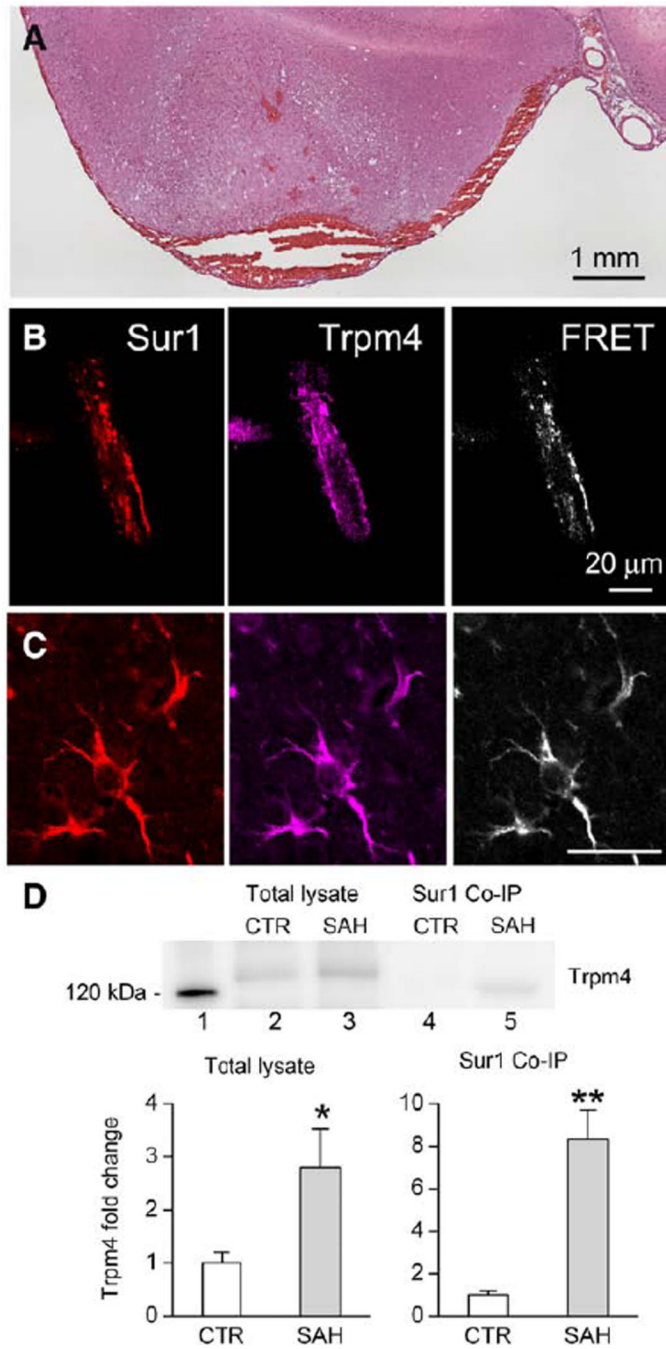


Figure 2. Sur1-Trpm4 channel in rat subarachnoid hemorrhage (SAH) shown by Förster resonance energy transfer (FRET) and coimmunoprecipitation. **A–C**, H&E-stained section (**A**) and immunolabeled sections (**B** and **C**) of rat entorhinal SAH; coimmunolabeled cortex shows coexpression of Sur1 and Trpm4 and FRET in elongated microvessels and astrocytes; representative of findings in 5 rats. **D**, Immunoblot (**top**) and densitometric analyses of immunoblots (**bottom**) for Trpm4 in rat entorhinal SAH; the immunoblot shows Trpm4 in total lysate (lanes 2, 3) and in the fraction immunoprecipitated using anti-Sur1 antibody (lanes 4, 5).

5); lane 1, molecular mass marker; the bar graphs give values for 4 replicates. *, $P<0.05$; **, $P<0.01$.

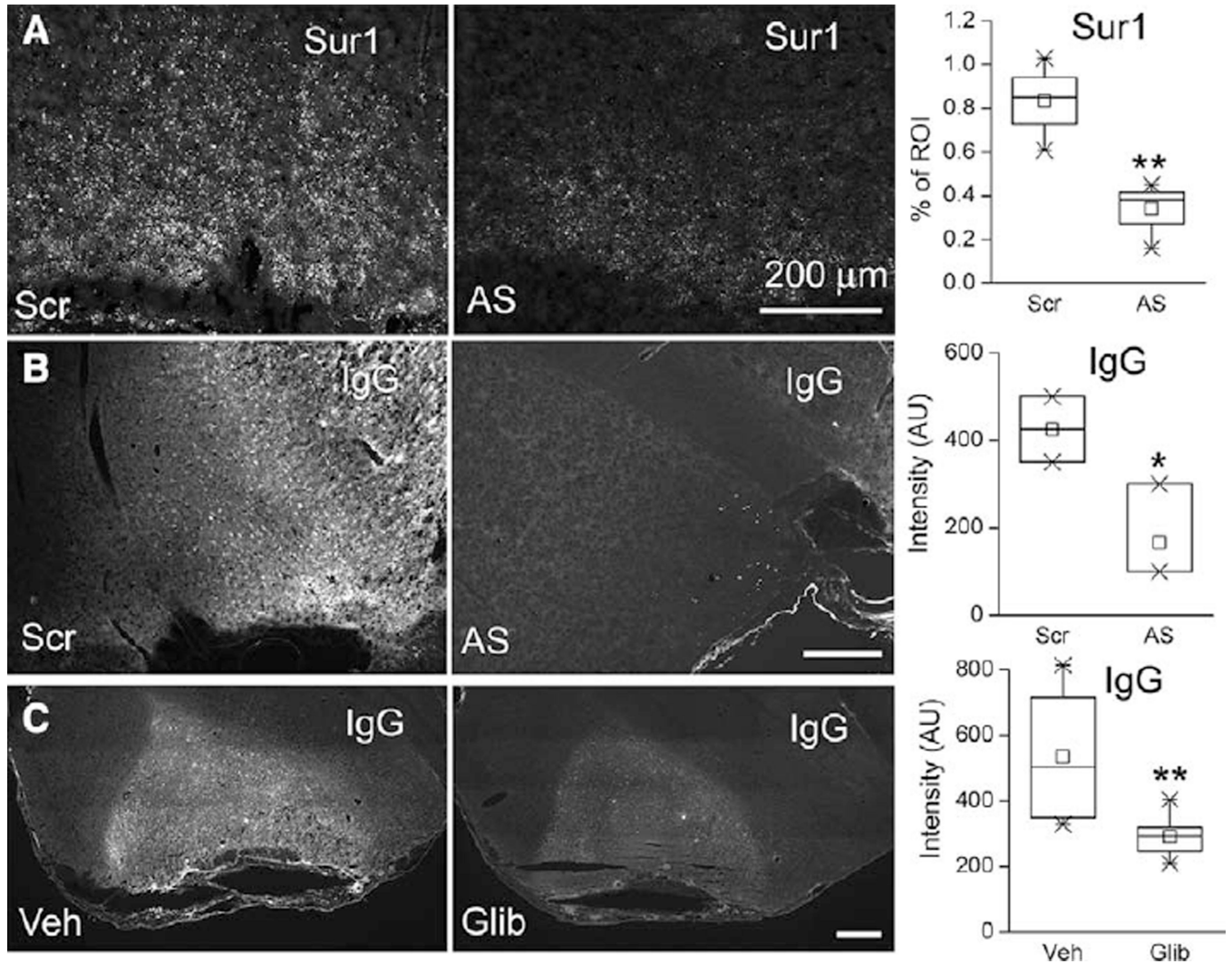


Figure 3. Antisense against *Abcc8* and glib-enclamide reduce immunoglobulin G (IgG) extravasation at 24 hours. **A** and **B**, Cortex adjacent to subarachnoid hemorrhage (SAH) immunolabeled for Sur1 (**A**) or IgG (**B**) from rats administered Scr-ODN or AS-ODN; box plots of quantitative analyses are shown; *, $P < 0.05$; **, $P < 0.01$; 3 rats per group; filament puncture model. **C**, Cortex adjacent to SAH immunolabeled for IgG from rats administered vehicle (Veh) or glibenclamide (Glib); box plots of quantitative analyses are shown; **, $P < 0.01$; 8 rats per group; entorhinal cortex injection model.

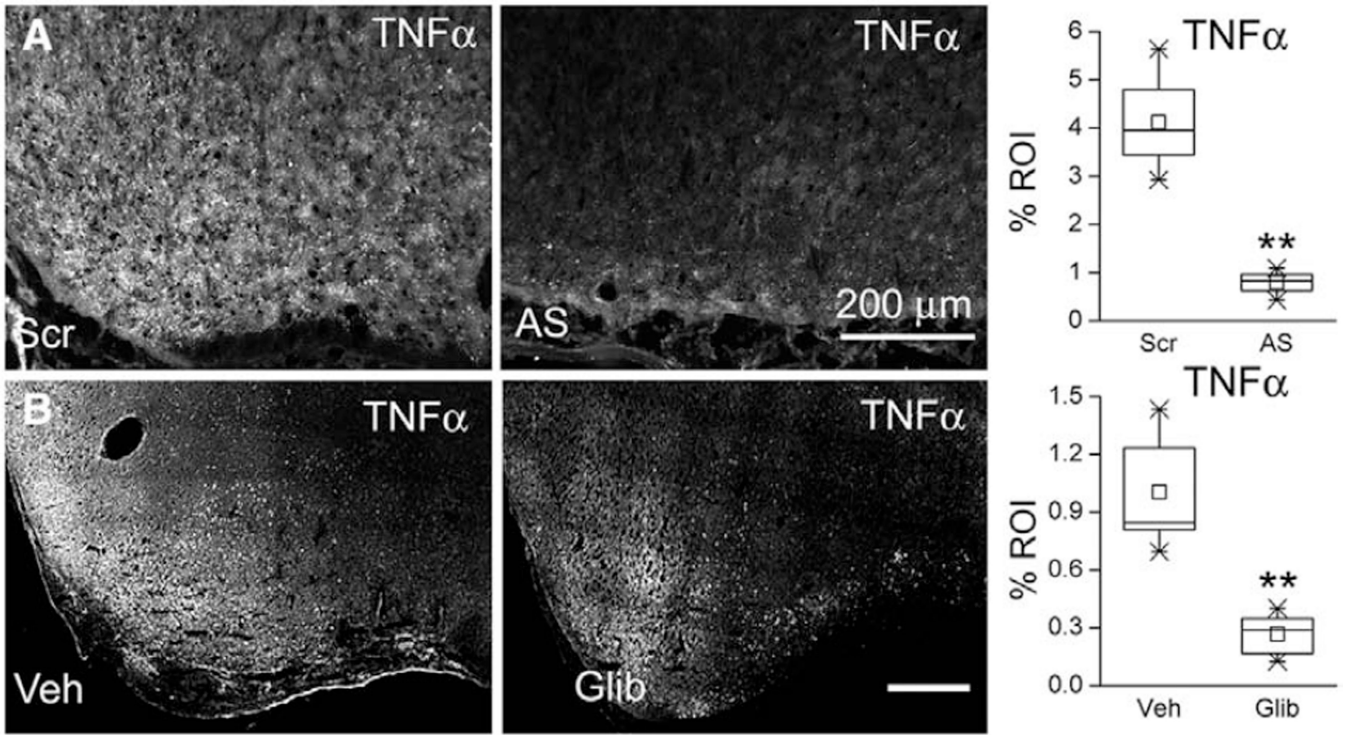


Figure 4.

Antisense against *Abcc8* and glibenclamide reduce tumor necrosis α (TNF α) overexpression at 24 hours. **A**, Cortex adjacent to subarachnoid hemorrhage (SAH) immunolabeled for TNF α from rats administered Scr-ODN or AS-ODN; box plots of quantitative analyses are shown; **, $P < 0.01$; same rats as in Figure 3A and 3B. **B**, Cortex adjacent to SAH immunolabeled for immunoglobulin G (IgG) from rats administered vehicle (Veh) or glibenclamide (Glib); box plots of quantitative analyses are shown; **, $P < 0.01$; the same rats as in Figure 3C.

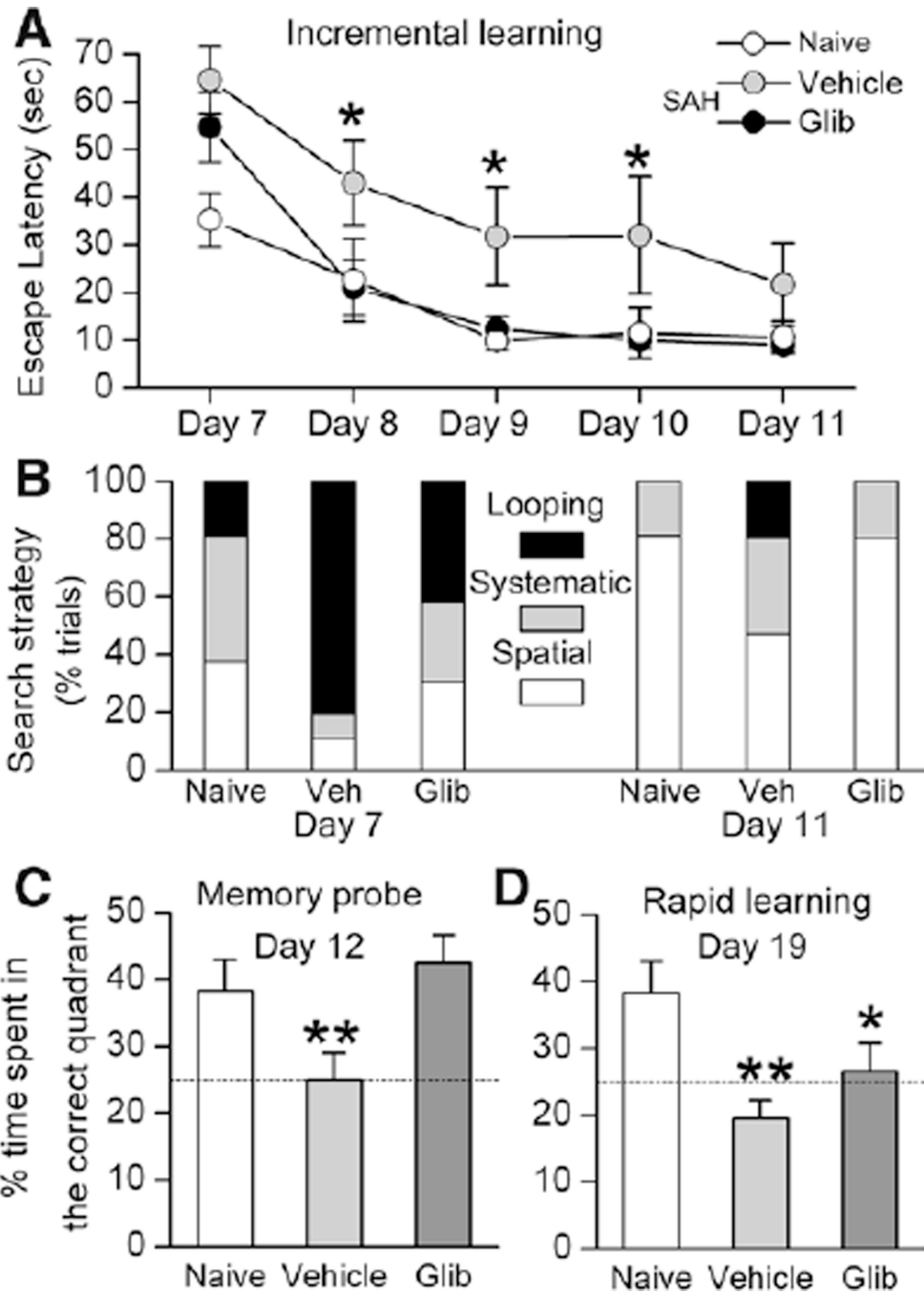


Figure 5. Glibenclamide reduces impairments in spatial learning and memory in rats with bilateral entorhinal SAH. **A** and **B**, Time spent searching for the submerged platform (**A**) and the percentage time spent in 1 of 3 platform search strategies (**B**) during incremental spatial learning in uninjured naïve controls (7 rats), and in rats with bilateral entorhinal SAH administered vehicle or glibenclamide (9 rats per group). **C** and **D**, Time spent in the correct quadrant during the memory probe (**C**) and during the test of rapid learning (**D**) in the same rats. *, $P < 0.05$; **, $P < 0.01$ comparing naïve with vehicle, or naïve with glibenclamide.

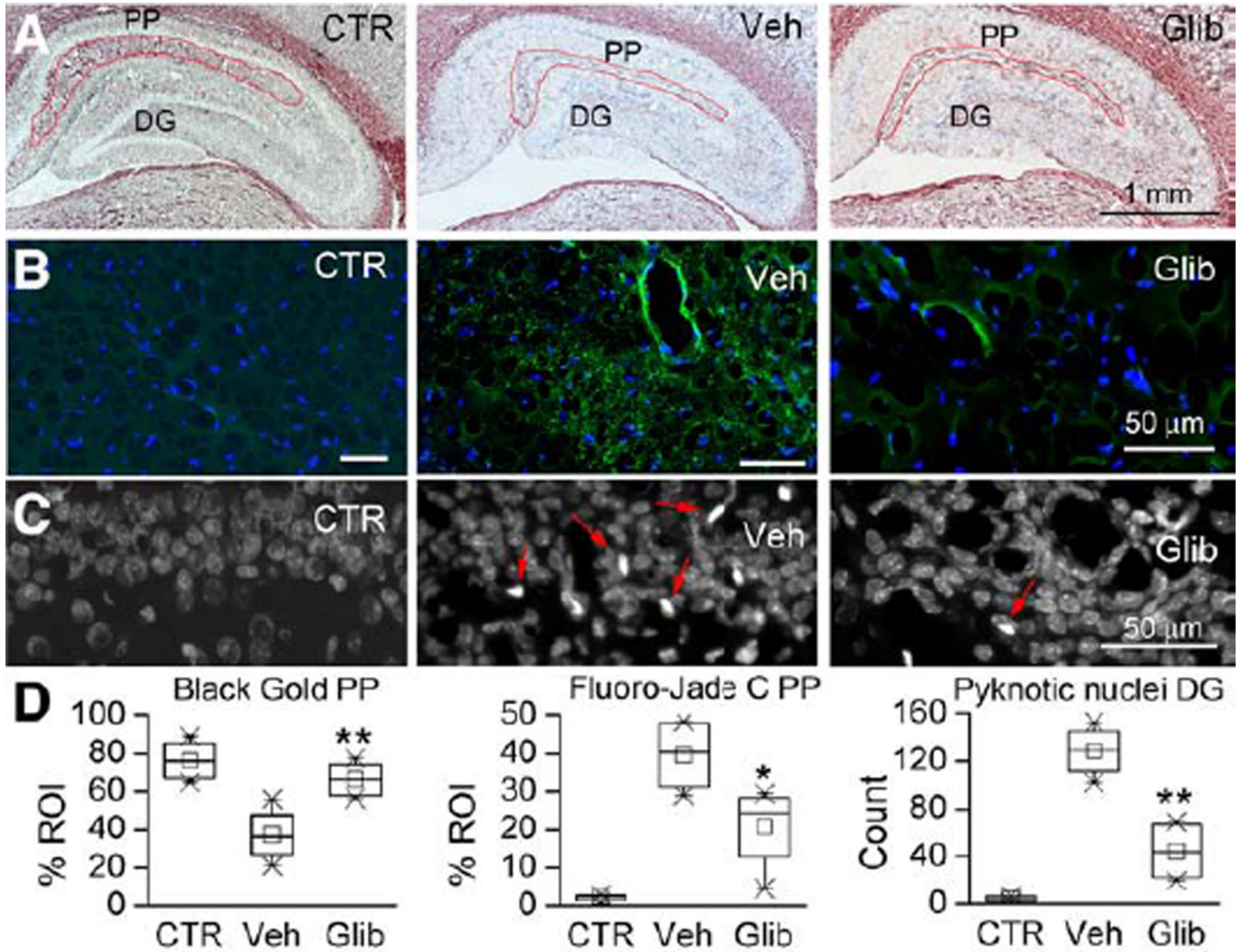


Figure 6. Glibenclamide reduces hippocampal tissue injury in rats with bilateral entorhinal subarachnoid hemorrhage (SAH). **A–C**, Hippocampi stained with Black Gold II (**A**), Fluoro-Jade C (**B**) or DAPI (**C**) from uninjured control rats (CTR), and rats with bilateral entorhinal SAH administered vehicle (Veh) or glibenclamide (Glib); in (**A**), the region of interest that was analyzed encompassing the perforant pathway (PP) is outlined; DG, dentate gyrus. **D**, Box plots of quantitative analyses of white matter labeling with Black Gold II in the PP, of cellular injury in the PP identified by Fluoro-Jade C staining, and of pyknotic nuclei in the DG of control rats and rats with entorhinal SAH administered vehicle or glibenclamide; 4 to 5 rats/group; *, $P < 0.05$; **, $P < 0.01$.